INFECTION AND IMMUNITY, June 1997, p. 2233–2239 Vol. 65, No. 6
0019-9567/97/$04.00+0

Prelytic and Lytic Conformations of Erythrocyte-Associated *Escherichia coli* Hemolysin

MAHTAB MOAYERI AND RODNEY A. WELCH*

Department of Medical Microbiology and Immunology, University of Wisconsin—Madison, Madison, Wisconsin 53706

Received 24 January 1997/Returned for modification 3 March 1997/Accepted 21 March 1997

Flow cytometry was developed as a method to assess the conformation of erythrocyte-bound *Escherichia coli* hemolysin polypeptide (HlyA). Topology of membrane-associated hemolysin ($HlyA^E$) was investigated by testing surface accessibility of HlyA regions in lytic and nonlytic bound states, using a panel of 12 anti-HlyA monoclonal antibodies (MAbs). Hemolysin associates nonlytically with erythrocytes at 0 to 2°C. To test the hypothesis that the nonlytic $HlyA^E$ conformation at 0 to 2°C differs from the lytic conformation at 23°C, MAb epitope reactivity profiles at the two temperatures were compared by flow cytometry. Four MAbs have distinctly increased reactivity at 0 to 2°C compared to 23°C. HlyA requires HlyC-dependent acylation at lysine residues 563 and 689 for lytic function. Toxin with cysteine substitution mutations at each lysine ($HlyA_{K563C}$ and $HlyA_{K689C}$) as well as the nonacylated form of hemolysin made in a HlyC-deficient strain were examined by flow cytometry at 0 to 2 and 23°C. The three mutants bind erythrocytes at wild-type toxin levels, but there are conformational changes reflected by altered MAb epitope accessibility for six of the MAbs. To test further the surface accessibility of regions in the vicinity of MAb-reactive epitopes, $HlyA^E$ was proteolytically treated prior to testing for MAb reactivity. Differences in protease susceptibility at 0 to 2° and 23°C for the reactivities of three of the MAbs further support the model of two distinct conformations of cell-associated toxin.

The *Escherichia coli* hemolysin is the prototype for study of structural and functional domains in the RTX family of toxins (24). This calcium-dependent toxin contains a cysteineless 110-kDa polypeptide (HlyA) and associates with a wide range of target cell types, causing lysis through membrane lesion formation (23). Little information is available on the conformation of soluble toxin, and until this study, no toxin-membrane topology investigations have been reported. In computer models of erythrocyte membrane-associated HlyA ($HlyA^E$) secondary structure, a hydrophobic N-terminal region (residues 178 to 410) is predicted to form eight transmembrane alpha-helical structures (2, 7, 13, 14). Although no experimental data for this structure exist, the functional toxin lesion has been attributed to a hypothesized pore formed by this structure based on loss of lytic activity by relevant HlyA deletion mutants (13, 14). Various functions are ascribed to the C-terminal half of HlyA, but there is no information on the conformation or membrane topology of these region. Within the C-terminal region, a series of glycine-rich, nine-amino-acid repeats (residues 721 to 848) bind calcium (4, 12), and the HlyC-dependent acylation (activation) of HlyA occurs at lysines 563 and 689 (9, 11, 22). It has been postulated that the acylated lysines aid in initial membrane association of the toxin (9).

Hemolysin can bind erythrocytes under conditions which do not lead to lysis. Four such conditions include association at 0 to 2°C, in dextran 4 buffer, in >1 mM Zn^{2+}, and under calcium-depleted conditions (1, 3, 15, 17). The conformation of erythrocyte-bound toxin potentially differs under each of these nonlytic states. It is hypothesized that binding to erythrocytes at 0 to 2°C represents a prelytic conformation, because with a shift to higher temperatures, erythrocytes begin to lyse, but only after a lag period (16). A late lytic conformation occurs with the $HlyA^E$ complex in the presence of dextran 4 (3, 17) or zinc (15), because removing either inhibitor results in immediate lysis. The purpose of this study was to investigate the membrane topology of $HlyA^E$ in order to discern if differences in conformation can be observed between the lytic and nonlytic states. Additionally, conformational changes hypothesized to occur in toxin when it is not acylated (HlyC-deficient variants) or potentially acylated at only one of the two lysine acylation sites were assessed. Flow cytometry was found to be a powerful method for the study of hemolysin binding to erythrocytes and assessment of conformational changes associated with different membrane-bound functional states.

MATERIALS AND METHODS

Bacterial strains and toxin preparation. WAM582(pSF4000) is a plasmid recombinant strain (DHI with *hlyCABD* in pACYC184) which has been previously described (25). WAM1824 is the source for wild-type toxin in most flow cytometry experiments. This strain is pWAM582(pSF4000) in the CL633 background (WAM1808) (5). The CL633 *E. coli* K-12 background strain results in approximately 20-fold-higher levels of HlyA production if *hlyA* is expressed from the complete *hly* operon compared to WAM582 expression. Cysteine substitution mutants were constructed by oligonucleotide-directed mutagenesis using the procedure of Kunkel (10). Mutations were subcloned into the *hly* operon as described elsewhere (18), and plasmid DNA was transformed into the CL633 background, resulting in WAM2197($HlyA_{K563C}$) and WAM2202($HlyA_{K689C}$). WAM783 is a $HlyC^-$ pro-HlyA construct of WAM582 and has been previously described (21). Bacteria were grown at 37°C in Luria-Bertani broth containing 20 μg of chloramphenicol per ml to an optical density at 600 nm of 0.75 to 0.85. Bacteria were pelleted, and culture supernatants passed through a 0.45-μm-pore-size Acrodisc were used as source of toxin.

Antibodies. Antibodies and their neutralization profiles have been initially described elsewhere (19). Epitopes for monoclonal antibodies (MAbs) G8, B7, and H10 have been further mapped by using a SPOTs kit (Genosys Technologies, The Woodlands, Tex.) (20). Epitopes for MAbs B9, G3, and D12 were further mapped by mutational analysis (20). Fluorescein isothiocyanate (FITC)-conjugated goat anti-mouse immunoglobulin G (IgG) and anti-rabbit IgG were purchased from Sigma Chemical Co. (St. Louis, Mo.).

Flow cytometry experiments. Sheep erythrocytes (sRBC) used as targets in all experiments were obtained fresh and defibrinated with glass beads. Toxin was associated with target cells by mixing 500 μl of a 0.5% (2.5×10^7 cells) sRBC suspension with 500 μl of toxin-containing culture supernatant and incubating the mixture for 30 min (room temperature) or 1 h (0 to 2°C), with occasional mixing. To prevent lysis in experiments performed at 23°C, all sRBC suspensions were made in dextran 4 buffer (30 mM dextran 4 [Serva Chemicals, Heidelberg, Germany] in 145 mM NaCl–45 mM KCl), and all washes were also performed in

* Corresponding author. Mailing address: Department of Medical Microbiology and Immunology, University of Wisconsin—Madison, 1300 University Ave., Madison, WI 53706. Phone: (608) 263-2700. Fax: (608) 262-8418. E-mail: rawelch@facstaff.wisc.edu.

A

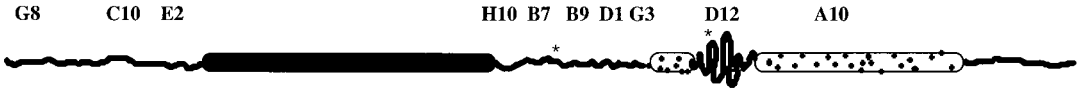

B

Antibody	Epitope Region	Concentration (mg/ml)	ELISA titer	IMMUNOBLOT titer	FC titer
Monoclonals					
G8	1-12	15.5	400	400	200
C10	1-161	13.2	1600	200	10/20
E2	161-194	9.4	400	800	20
H10	512-524	9.2	102,400	102,400	1000
B7	518-530	20	409,600	10,000	1000
B9	594-614	9.4	400	200	100
D1	626-640	19.5	409,600	5000	1000
G3	626-640	14.8	409,600	5000	1000
D12	684-696	NA	500	500	50
A10	745-829	NA	5000	5000	100
B10	Conformational	8	100	200	10
C7	Conformational	10	100	200	10
Polyclonal					
212	multiple	NA	409,600	102,400	1000

FIG. 1. (A) Schematic of HlyA showing structural regions and MAb epitopes. Designations and locations of MAb epitopes are shown above the horizontal bar. The thickest straight black region indicates the putative transmembrane domain. The open dotted region represents the calcium-binding repeats of HlyA, interrupted by the modification region containing acylation site lysine 689 and the D12 acylation-dependent epitope. Acylation sites are shown with asterisks at residues 563 and 689. (B) Epitope regions and concentrations of MAbs and the maximum HlyA detection titers by ELISA and immunoblotting (19, 21). FC titer is the dilution used in the primary antibody binding step of flow cytometry experiments.

this buffer. Dextran 4 buffer prevents hemolysin-induced lysis of erythrocytes by osmotic protection (3, 17). Erythrocytes with bound hemolysin (E^{HlyA}) were washed twice to remove unbound toxin and resuspended in 100 μl of dextran buffer. Anti-HlyA monoclonal or polyclonal primary antibodies were added (dilutions are given in Fig. 1B) and incubated for 1 h. Erythrocytes were washed twice with 500 μl of buffer to remove unbound primary antibody, resuspended in 100 μl of 1:25-diluted FITC-conjugated goat anti-mouse or anti-rabbit IgG (Sigma), and incubated in the dark for 30 to 45 min. Cells were washed once in buffer and resuspended in 300 μl of dextran buffer prior to analysis. Samples at 0 to 2°C were prepared in a similar fashion, in an ice water-ethanol bath with the following variations: sRBC suspensions, antibody dilutions, and washes utilized cold saline instead of dextran 4. Centrifugation was limited to 5 s, and experiments were performed in a cold (4°C) room. Samples were maintained at 0 to 2°C in 300 μl of cold saline until the time of analysis. Erythrocytes were assessed for fluorescein-specific fluorescence with a FACStar flow cytometer (Becton Dickinson, Mountain View, Calif.), and 5,000 or 10,000 events were collected per sample. Mathematical analysis of data was performed by using the PCLYSIS flow cytometry analysis software program (Becton Dickinson). The negative controls in these experiments were E^{HlyA}; E^{HlyA} plus primary antibody; E^{HlyA} plus secondary (FITC-conjugated) antibody; and E^{HlyA} plus two irrelevant primary antibodies plus secondary (FITC-conjugated) antibody.

Proteolysis experiments. The relative susceptibility of each MAb epitope to proteolytic treatment was investigated for $HlyA^E$ to support the topological location relative to the erythrocyte membrane or identify a proteolytically resistant structure. Experiments were performed as described above, with modifications: After association of toxin with erythrocyte targets and removal of unbound toxin, cells were resuspended in 0.5 ml of dextran buffer (23°C) or saline (0 to 2°C) and treated with 20 μl of a proteolytic cocktail (trypsin XII.S-chymotrypsin VII-proteinase K [Sigma], each at 250 μg/ml). Proteolysis was carried out at either temperature for 15 to 30 minutes. Erythrocytes were washed four times with 1 ml of dextran buffer or cold saline to remove proteases prior to resuspension in 100 μl of dextran buffer or cold saline and addition of primary antibody. Negative controls included protease-treated erythrocytes with no toxin associated, as well as those listed above.

RESULTS

Detection of hemolysin bound to erythrocytes by flow cytometry. The first goal in these studies was to establish if flow cytometry could be used as a method to measure toxin binding to target cells. Polyclonal anti-HlyA antibodies were used to detect binding of wild-type hemolysin to dextran 4-protected erythrocytes at ambient temperature. Eighty to 90% of all E^{HlyA} bind polyclonal antibody. Similar experiments were performed with nonacylated hemolysin and with cysteine substitution mutants ($HlyA_{K563C}$ and $HlyA_{K689C}$). $HlyA_{K563C}$ has a 300-fold decrease in hemolytic activity, while non-acylated HlyA and $HlyA_{K689C}$ have no hemolytic activity (18). All three mutant toxins bind erythrocytes at both 0 to 2 and 23°C, as indicated by polyclonal binding. Figure 2 shows a representa-

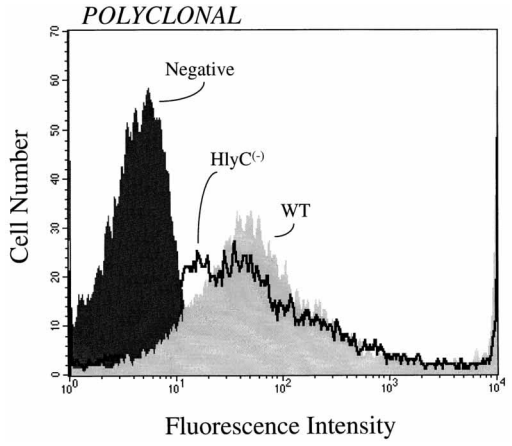

FIG. 2. Wild-type toxin and nonacylated, pro-HlyA bind erythrocytes. Results of a representative experiment show the binding of equivalent amounts of toxin from WAM783 ($HlyC^-$ pro-HlyA) and WAM582 (wild type [WT]). Anti-hemolysin polyclonal antibody (1:1,000) was used to detect binding. The negative control is toxin-bound erythrocytes plus secondary FITC-conjugated antibody. All other negative controls (described in Materials and Methods) showed lower levels of fluorescence than this control. For each sample, 10,000 collected cells were assessed by flow cytometry.

TABLE 1. Percentage of toxin-bound erythrocytes showing reactivity with each antibody at 0 to 2 and 23°C[a]

Antibody	Wild type		K689C		K563C		HlyC$^-$	
	23°C	0–2°C	23°C	0–2°C	23°C	0–2°C	23°C	0–2°C
G8	70 ± 4	77 ± 3	21 ± 16	–	22 ± 2	–	32 ± 4	ND
C10	–	52 ± 5	–	–	–	I	–	I
E2	–	–	–	–	–	–	–	–
H10	–	–	–	–	–	–	–	–
B7	–	54 ± 9	17 ± 10	I	–	–	–	44 ± 14
B9	80 ± 3	92 ± 2	82 ± 2	75 ± 4	51 ± 9	51	26 ± 18	I
D1	62 ± 6	66 ± 11	64 ± 3	64 ± 9	55	45	39 ± 4	34
G3	83 ± 2	75 ± 3	72 ± 6	78 ± 4	42	36	84 ± 3	ND
D12	–	–	–	–	–	–	–	–
A10	–	–	–	–	–	–	–	ND
B10	–	60 ± 11	18 ± 14	46	–	–	–	28 ± 11
C7	15 ± 3	55 ± 8	22 ± 1	I	–	–	14 ± 8	ND
Polyclonal	88 ± 2	95 ± 2	85 ± 4	85 ± 5	54	49	59 ± 15	54 ± 14

[a] Values represent the percentages of erythrocytes with fluorescence greater than that of negative controls. Negative controls are described in Materials and Methods. For experiments performed with wild-type toxin, $n = 19$ at 23°C and $n = 5$ at 0 to 2°C; for all other experiments, $n = 2$ to 4. –, <10% of E^{HlyA} show fluorescence levels greater than that of negative controls; ND, experiment not done; I, inconclusive.

tive experiment depicting the binding of wild-type hemolysin and nonacylated toxin to erythrocytes.

MAb epitope accessibility and $HlyA^E$ topology. To test the hypothesis that certain regions of $HlyA^E$ are membrane inserted while other regions are surface exposed, a panel of well-defined MAbs with epitopes throughout the toxin was used to probe the accessibility of different HlyA domains in toxin bound to erythrocytes (Fig. 1). These antibodies react with HlyA in its native soluble conformation, as indicated by enzyme-linked immunosorbent assay (ELISA) and native dot blots, as well as to its putatively denatured state in immunoblotting (19, 21) (Fig. 1). E^{HlyA} protected from lysis by dextran 4 buffer was tested for reactivity with each MAb at 23°C. Distinctly positive and negative reactions are observed with the each MAb (Table 1; Fig. 3). The exception is MAb C7, which reacts with a conformational epitope and can give no reactivity or up to 15% reactivity (19, 21). MAb G8 with an epitope in the first 12 residues of the toxin binds a large percentage of E^{HlyA}, which indicates surface exposure of the N terminus of HlyA in its lytic bound state. Interestingly, MAbs C10 and E2, with epitopes just downstream of this region, and closer to the putative transmembrane domain, are nonreactive. MAbs D12 and A10 do not bind to E^{HlyA}, indicating that the acylated lysine 689 region and downstream calcium-binding repeats are topologically unavailable to antibody probes. The region between the putative transmembrane domains and calcium-binding repeats contains five MAb epitopes with interesting contrasts in reactivity. While MAbs B9, D1, and G3 bind 80% of all E^{HlyA}, MAbs B7 and H10, with overlapping and adjacent epitopes located only 60 residues N terminal to the B9 epitope, show no reactivity with $HlyA^E$ (Table 1). The lysine 563 acylation site of HlyA lies between the inaccessible B7 epitope and the readily reactive B9 epitope region. Antibodies with conformational epitopes (B10 and C7) usually showed no binding to E^{HlyA}; however, as mentioned above, there was an inconsistent low reactivity seen with MAb C7 (Table 1).

Altered MAb reactivity profiles indicate conformational differences in $HlyA^E$ at 0 to 2°C. To test the hypothesis that the prelytic membrane-bound conformation of toxin at 0 to 2°C differs from its lytic conformation at higher temperatures, MAb binding to E^{HlyA} at 0 to 2°C was compared to that at 23°C (Table 1). The results indicate a striking increase in the percentage of E^{HlyA} reacting with MAbs B7, C10, and B10 which were nonreactive at 23°C (Fig. 3C and D). There is also a consistent positive reactivity for MAb C7, which has a variable, low level of reactivity at 23°C. These results clearly indicate a different conformation for the nonlytic bound toxin at 0 to 2°C. None of the epitope regions that were surface exposed at 23°C lose reactivity under the 0 to 2°C binding conditions (Fig. 3B). This general increase in epitope availability indicates that more regions of toxin are surface exposed under the 0 to 2°C conditions. MAbs A10, D12, E2, and H10 remain nonreactive at the lower temperature (Fig. 3A).

MAb reactivity profiles for $HlyA_{K563C}$, $HlyA_{K689C}$, and nonacylated pro-HlyA. The acylation-defective HlyA mutants were tested in flow cytometry experiments at 0 to 2 and 23°C (Table 1; Fig. 3). Similar to results seen with wild-type toxin, MAbs A10, D12, E2, and H10 show no reactivity with the mutant toxins bound to erythrocytes at either tested temperature (Fig. 3A). MAb D1 is the only antibody that shows consistent positive reactivity with all three erythrocyte-bound mutants at both temperatures (Fig. 3B). In contrast to results with wild-type toxin, a small percentage of cells bound with $HlyA_{K689C}$ showed low reactivity with MAbs B7, B10, and C7 at 23°C (Fig. 3D). Additionally, a significantly lower percentage of erythrocytes with $HlyA_{K689C}$ bound react with MAb G8, and this reactivity is lost at 0 to 2°C. $HlyA_{K563C}$ shows the same lowered reactivity with MAb G8 at both temperatures. All other reactivities for this mutant at 23°C indicate a reactivity profile similar to that for wild-type toxin, but with only 40 to 50% of the E^{HlyA} population having antibody-reactive sites on their surface, in contrast to the 70 to 90% seen with wild-type toxin (Table 1). Interestingly, $HlyA_{K563C}$ does not increase in the number of accessible MAb epitopes at 0 to 2°C. Its overall reactivity profiles are similar at the two temperatures (Table 1). Nonacylated pro-HlyA also shows altered MAb reactivities (Table 1). The striking result with this particular mutant is the lowered reactivity seen for MAb B9. It is clear from these observations that the mutant toxins bind erythrocytes with conformations different from that of the wild type at both 0 to 2 and 23°C.

Susceptibility of accessible surface-exposed epitopes of $HlyA^E$ to proteolytic treatment. To further test the surface exposure of positive-reacting MAb epitope regions and to investigate local conformational structure in the vicinity of these epitopes, $HlyA^E$ was treated with proteases prior to assessing MAb reactivity profiles. The reactivities for three of five reactive MAbs (B9, C7, and D1) are completely eliminated from

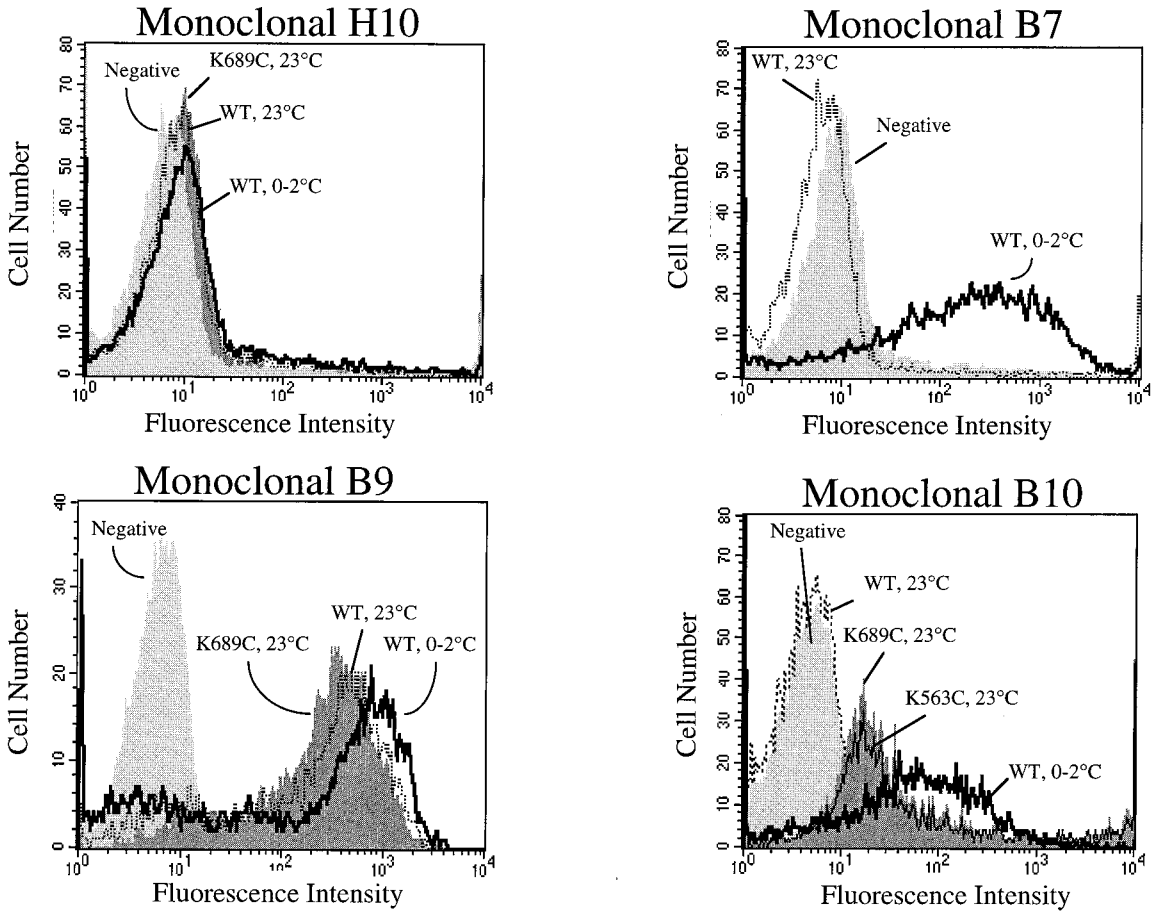

FIG. 3. Representative MAb reactivity profiles for wild-type and mutant toxin bound to erythrocytes at 0 to 2 and 23°C. (A) Lack of reactivity of MAb H10 (epitope $HlyA_{512–524}$) with wild-type (WT) toxin bound to erythrocytes under nonlytic (0 to 2°C) and lytic (23°C) conditions, as well as negative reaction with mutant Hly_{K689C}; (B) positive reaction with MAb B9 (epitope $HlyA_{594–614}$) in similar experiments; (C) Experiment where a distinct change in reactivity with MAb B7 is seen at the two experimental temperatures; (D) availability of the MAb B10 conformational epitope at 0 to 2°C and its loss at 23°C, plus a representative experiment where a mutant toxin shows B10 reactivity different from that of wild-type toxin. The negative control is E^{HlyA} plus irrelevant primary antibody plus secondary FITC-conjugated antibody. All other negative controls (described in Materials and Methods) showed lower levels of fluorescence than this control. Data are for 10,000 collected cells per sample.

more than 50% of all E^{HlyA} at 23°C (Table 2; Fig. 4B). At 0 to 2°C, the reactivities of five of eight of the normally positive MAbs (B7, B10, C10, D1, and G8) are abrogated by proteolytic treatment (Table 2). The remaining 10 to 35% of proteolytically treated E^{HlyA} which retain reactivity with these MAbs show a 10- to 500-fold reduction in fluorescence intensity. This is a measure of the number of reactive epitopes per cell. The readily reactive epitopes for MAbs B9 and G3 are not susceptible to protease treatment at 0 to 2°C but are easily removed by proteolysis at 23°C. The G3 epitope is also relatively resistant to protease treatment at 23°C (Fig. 4A).

The N-terminal epitope region for MAb G8 is protease sensitive in the nonlytic conformation at 0 to 2°C (Table 2). In the lytic conformation, its MAb reactivity with proteolytically treated E^{HlyA} is reduced up to 10-fold in terms of fluorescence intensity. Although this result indicates that a lower number of MAb-reactive sites exist per erythrocyte, all E^{HlyA} cells maintain toxin molecules with accessible MAb G8-reactive epitopes and the overall percentage of positive-reacting cells is unchanged (Fig. 4C). In this context, it is important to emphasize that the values in Table 2 represent the percentages of E^{HlyA} for which proteolytic treatment results in complete loss of a particular epitope; reductions in fluorescence intensity that do

TABLE 2. Loss of epitope regions and MAb reactivity with proteolytic treatment

Antibody	Avg % sRBC with MAb epitope removed by proteolysis ± SD[a]	
	23°C	0–2°C
G8	4 ± 2	63 ± 20
C10	NA	90 ± 6
E2	NA	NA
H10	NA	NA
B7	NA	45 ± 16
B9	66 ± 10	5 ± 2
D1	80 ± 15	66 ± 7
G3	18 ± 14	1 ± 1
D12	NA	NA
A10	NA	NA
B10	NA	70 ± 20
C7	100 ± 0	I

[a] Average percentage of erythrocytes showing loss of MAb reactivity (fluorescence) when $HlyA^E$ is treated proteolytically. $n = 3$ for all experiments except for MAbs G3, G8, and B9 ($n = 4$ to 6). NA, not applicable (MAb is nonreactive for $HlyA^E$ with or without proteolytic treatment); I, inconclusive due to inconsistent results.

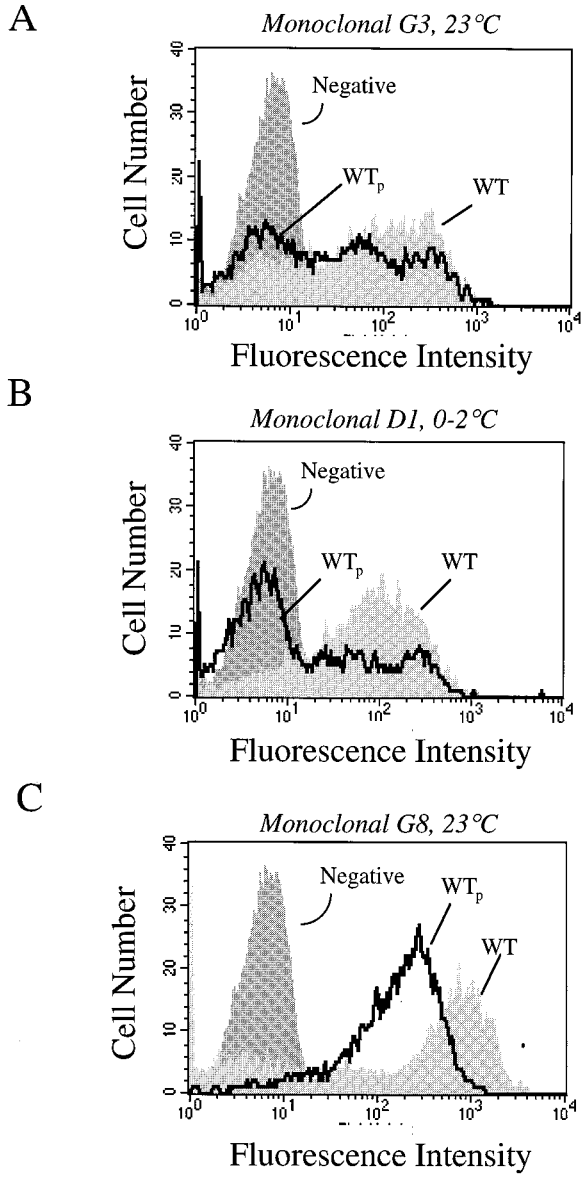

FIG. 4. Representative MAb reactivity profiles with wild-type proteolytically treated (WT_p) and untreated (WT) $HlyA^E$ at 0 to 2 and 23°C. (A) Proteolytic treatment of $HlyA^E$ does not alter reactivity with a MAb epitope (G3) at 23°C; (B) proteolytic treatment of E^{HlyA} removes a MAb epitope (D1) from 90% of erythrocytes at 23°C; (C) A MAb (G8) shows reduced reactivity with protease-treated $HlyA^E$ but remains reactive with all the erythrocytes. Data are for 5,000 collected cells per sample.

not result in removal of all available epitopes on an erythrocyte are not represented by the values reported in this table.

DISCUSSION

Prior to these studies, the structural and functional domains of the soluble and membrane-associated forms of the *E. coli* hemolysin were postulated from amino acid sequence algorithms and genetic studies (7, 8, 12–14). In this study, flow cytometry methods were used to make several significant observations about the topology of $HlyA^E$. First, some but not all anti-HlyA MAb epitopes which are available for MAb binding on the soluble form of the toxin are missing once the toxin is stably associated with an erythrocyte. Second, the hemolysin-erythrocyte complex can be shifted from a prelytic state to a lytic one where additional MAb epitopes become unavailable for binding. Toxin association with erythrocytes at 0 to 2°C is characterized as a prelytic state, because following a shift to 23°C there is a lag period before lysis begins. This situation is in contrast to the immediate lysis that occurs at 23°C, when an osmotic protectant such as dextran 4 is removed from an E^{HlyA} suspension. Thus, the lytic structure of $HlyA^E$ in these studies represents a functionally mature complex achieved at 23°C in the presence of a protectant such as dextran 4. We postulate that the prelytic and lytic states of hemolysin, as well as association of toxin with erythrocytes under nonlytic conditions (calcium-free conditions; nonacylated or mutant toxins) represent independent membrane-bound HlyA conformations. In this study, flow cytometry was used to study conformations of prelytic and lytic wild-type $HlyA^E$ as well as the erythrocyte-membrane associated nonacylated toxin and two HlyA acylation mutants.

In the lytic state, at 23°C, MAbs tested for reactivity with E^{HlyA} show distinct positive and negative reactivities in a manner completely independent of and often in contrast to their immunoblot, native dot blot, and ELISA HlyA titers (Fig. 1). Thus, the flow cytometry results reported here do not reflect differences in the titer of MAb used to detect either the native or denatured soluble form of HlyA. Of the 12 MAbs that react with soluble HlyA, only 4 react with $HlyA^E$ in the lytic state at 23°C. The MAb reactivity profiles indicate surface accessibility of the HlyA N terminus and the region between residues 594 and 640 ($HlyA_{594–640}$). MAb G8 reacts with $HlyA^E$, and its epitope lies within the first 12 residues of HlyA. MAbs B9, D1, and G3 also react, and their epitopes exist within $HlyA_{594–640}$. The eight nonreactive MAbs indicate that regions directly N terminal and C terminal to residues 594 to 640 are inaccessible for MAb reactivity. Domains which contain nonreactive MAb epitopes include regions on either side of the putative transmembrane domain and just N-terminal to the 563 acylation site, the 689 acylation site region, and the repeat region. The lack of reaction with epitopes within these domains could reflect membrane insertion and lack of surface accessibility for the associated regions. Alternatively, it is also possible that local protein folding in the vicinity of the tested epitope prevents MAb accessibility. Unfortunately, at present there are no MAbs available for the putative transmembrane region or the C-terminal $HlyA_{800–1023}$ region.

While the four positive reacting MAbs are also reactive in the prelytic state, four additional MAbs react with $HlyA^E$ at 0 to 2°C. MAb C10 reacts to an epitope in the N terminus which is accessible at 0 to 2°C, in contrast to its inaccessibility at 23°C. A striking MAb reactivity difference between the lytic and prelytic bound states is the positive reactivity of the B7 epitope at 0 to 2°C, because a directly adjacent epitope with very strong immunoblot and ELISA titers (MAb H10) remains inaccessible at this temperature. Because of its proximity to the B7 epitope, we believe that reactivity to the H10 epitope is occluded by local folding in a manner that results in inaccessibility at both 0 to 2 and 23°C, rather than insertion within the erythrocyte membrane. MAbs B10 and C7, which react against a conformational epitope, are nonreactive at 23°C. MAb C7 does show slight reactivity at this temperature but in an inconsistent manner, suggesting the epitope is within or near a dynamic structure. What is striking is that at 0 to 2°C, both MAb B10 and MAb C7 consistently react to $HlyA^E$. It is difficult to assess the particular conformational changes associated with the reactivities of MAbs B10 and C7, but we can conclude that these epitopes are stable in the prelytic state of bound toxin. In the lytic state, however, the epitopes are de-

stroyed, membrane embedded, or surface exposed but in an inaccessible conformation. We conclude that distinct structural differences exist in the N terminus of the toxin, as well as in the $HlyA_{518–530}$ region between the prelytic and lytic states of bound toxin. Regions in proximity of epitopes for MAbs E2, H10, A10, and D12 are inaccessible at both experimental temperatures.

We hypothesized that changes in the acylation status of the hemolysin would be reflected by differences in MAb reactivity between the wild-type toxin and different HlyA mutants directly affected in acylation. First, we confirmed the recent observation that nonacylated pro-HlyA does stably associate with erythrocytes (1). The same can be said of the HlyA mutants which are substituted with cysteines at either of the known sites of acylation ($HlyA_{K563C}$ and $HlyA_{K689C}$). The MAb reactivity profiles for $proHlyA^E$ and especially $HlyA_{K563C}{}^E$ indicate a generally lower percentage of erythrocytes with MAb-reactive species bound than seen with $HlyA^E$, and at first glance this may be attributed to a general reduced binding to erythrocytes. We do not favor this conclusion, however, because if the $HlyA_{K563C}$ mutant is directly fluoresceinated at the cysteine residue, bound to erythrocytes, and analyzed by flow cytometry, it shows binding levels similar to those for the wild-type toxin (18). Therefore, we prefer an argument that an equal number of mutant toxin molecules bind erythrocytes, but many are simply not detected with antibodies for unknown reasons. We also cannot draw any conclusions on the structural basis for the overall lower reactivity seen with $proHlyA^E$ and $HlyA_{K563C}{}^E$ compared to $HlyA^E$.

More MAbs react with $HlyA_{K689C}{}^E$ at 23°C than with $HlyA^E$. MAbs B7 and B10 react with the $HlyA_{K689C}{}^E$ at this temperature but not with $HlyA^E$. It is very interesting that the G8 epitope has poor accessibility at 23°C and is not accessible at 0 to 2°C in both $HlyA_{K563C}{}^E$ and $HlyA_{K689C}{}^E$ structures, whereas it is readily available for $HlyA^E$ at both temperatures. This finding indicates that a change in the covalent structure of HlyA at position 563 or 689 causes a local change in $HlyA^E$ structure involving the very N-terminal 12 amino acids. Perhaps the most striking conformational change occurs in the middle of the toxin, covering the B9 epitope at $HlyA_{594–614}$. In the prelytic conformation at 0 to 2°C, HlyA and either of the lysine substitution mutants react with MAb B9. However, MAb B9 reacts poorly and inconsistently with $pro\text{-}HlyA^E$ at 0 to 2°C as well as 23°C.

The B7, C7, and C10 epitope regions show inconsistent reactivities at 0 to 2°C for all three mutants. Inconsistent reactivity is defined as a situation where a MAb shows a widely different range of reactivities in separate experiments, ranging from no to very high reactivity. These three epitopes were shown to have distinct and stable contrasting reactivities with the wild-type toxin in its prelytic and lytic states. We cannot explain the structural basis for the inconsistency seen in MAb reactivities for these epitopes in the mutants. The only MAbs for which consistent reactivity was seen in all experiments were the nonreactive MAbs A10, E2, D12, and H10.

Proteolytic treatment of wild-type $HlyA^E$ prior to testing of MAb reactivities indicated that in most cases, epitopes are totally removed from more than 50% of E^{HlyA}, accompanied with 10- to 500-fold reduction in the fluorescence intensity on the remaining E^{HlyA}. The level of fluorescence intensity indicates the number of available epitopes per cell. None of the normally nonreactive MAbs H10, E2, D12, and A10 became reactive with proteolytic treatment. A fascinating result seen in these experiments is that the $HlyA_{594–640}$ region containing the B9 and G3 epitopes appears resistant to proteolysis at 0 to 2°C. The region containing these epitopes is surface exposed at both temperatures and proteolytically sensitive at 23°C; therefore, it is also expected to be sensitive at 0 to 2°C. These results indicate an altered local folding of this domain at 0 to 2°C. Curiously, MAb G3 reacts to the same $HlyA_{626–639}$ region (AGSANIYAGKGHDV) as MAb D1 does. MAb D1, however, can no longer react to proteolytically treated $HlyA^E$. Based on this difference in proteolytic susceptibility, we hypothesize that the G3 epitope is N terminal to the D1 epitope, with the D1 epitope potentially involving the $HlyA_{K635}$ trypsin digestion site.

In recent investigations, we used site-specific fluorescein-labeled cysteine substitution mutants of HlyA in conjunction with flow cytometry to discover that residues 344, 369, 479, 563, 578, 689, 696, and 913 cannot be proteolyzed from $HlyA^E$ at either 0 to 2 or 23°C (18). These residues are not within the reactive MAb regions studied here, although two sites (563 and 578) fall between the B9 and B7 epitopes. Both of these epitopes are fully accessible at 0 to 2°C, while B7 is inaccessible at 23°C. The regions covering residues 563 and 578 are also resistant to proteolysis at 0 to 2°C. We conclude that the 563 acylation region, similar to the 689 lysine acylation site, does not become accessible at either temperature, despite the altered conformation and accessibility of the directly N-terminal B7 epitope region at the two temperatures.

The only proteolytically susceptible tested fluorescein-labeled residue was amino acid 131 in the prelytic structure of $HlyA^E$. The epitope for MAb C10 lies close to this site and is also proteolytically removed at 0 to 2°C. In the lytic state, the C10 epitope is nonreactive and the 131 site is not proteolyzed from $HlyA^E$. These complementary findings provide evidence for distinct changes in the conformation and accessibility of the N terminus of HlyA in its prelytic and lytic membrane-bound conformations and further validate flow cytometry analyses of $HlyA^E$ topology.

Model of $HlyA^E$ topology. Based on the results presented here, models of the topology of HlyA in erythrocyte membranes in prelytic and lytic states can be derived, but there are several caveats to be discussed. The lack of MAb reactivity to an epitope present in an integral membrane protein could be the result of occlusion of the epitope by protein folding, modification, or interaction with another protein. These factors are as likely to cause loss of reactivity to an epitope as its insertion within the erythrocyte membrane. These same topological constraints could also result in loss of proteolytic sensitivity at any particular site of a membrane-associated protein. For simplicity, our models will describe lack of MAb reactivity or protease sensitivity of a region in terms of protection by membrane insertion, although it is clear that more complicated molecular explanations are likely. Regardless of actual HlyA topology relative to the target membrane, the differences observed in MAb reactivity observed in these investigations for the different states of associated toxin do indicate distinct conformation states. Two main regions of HlyA change in surface accessibility between the prelytic and lytic states. One is the $HlyA_{12–131}$ region and the other is the $HlyA_{518–530}$ region.

For the $HlyA^E$ lytic state, the results presented here support the hypothesis that the large 350-amino-acid region C terminal to $HlyA_{S131}$ is membrane inserted. Acylation site $HlyA_{K563}$ and the region surrounding it are also inserted. Between $HlyA_{K563}$ and another inserted area surrounding acylation site $HlyA_{K689}$, the $HlyA_{584–640}$ region is exposed on the external side of the erythrocyte membrane. This region is predicted to have the highest probability of surface exposure by different computer algorithms (21). The lack of A10 reactivity for $HlyA^E$ suggests that the calcium binding repeat region is embedded in the membrane. This result is consistent with the

observation made with the small NodO RTX exoprotein (6). The NodO protein essentially consists of only the repeat-like sequence and can insert and form pores in artificial lipid bilayers (6).

The model for the prelytic $HlyA^E$ complex predicts two surface-exposed areas which become membrane inserted in a temperature-dependent fashion to achieve the mature lytic conformation of $HlyA^E$. The N-terminal $HlyA_{12-131}$ region and central $HlyA_{518-530}$ region are external to the membrane in the prelytic $HlyA^E$ state. In the fully competent lytic $HlyA^E$ complex, these two regions become embedded within the membrane-toxin structure. The observation that the acylation status of HlyA has conformation consequences in the N-terminal region of $HlyA^E$ provides striking evidence that acylation has global rather than a simple local impact on the structure and function of hemolysin.

Application of flow cytometry methods in the study of RTX toxins against nonerythrocyte cell types is an important next step in the RTX field. Preliminary studies of the association of HlyA with and its cytotoxicity against Raji and BL-3 cell lines indicate MAb reactivity profiles different from what is reported here for erythrocytes. Additionally, our studies on the association of other RTX toxins with different target cells show a lack of correlation between toxin binding and target cell susceptibility. We believe that the flow cytometry techniques applied in this study represent a powerful new tool for the study of conformations associated with target-bound hemolysin and will help dissect the steps associated with the lytic process induced by this toxin in membranes.

ACKNOWLEDGMENTS

We thank Shai Pellett for mapping MAb epitopes. We thank Kathleen Schell and Kristen Elmer of the UW Cancer Center Flow Cytometry facility for help with flow cytometry experiments. We also thank Luella Babaayee for providing sRBCs.

This work was supported by Public Health Service grant AI20323.

REFERENCES

1. **Bauer, M. E., and R. A. Welch.** 1996. Association of RTX toxins with erythrocytes. Infect. Immun. **64:**4665–4672.
2. **Benz, R., A. Dobereiner, A. Ludwig, and W. Goebel.** 1992. Haemolysin of *Escherichia coli*: comparison of pore-forming properties between chromosome and plasmid-encoded haemolysins. FEMS Microbiol. Immunol. **5:**55–62.
3. **Bhakdi, S., and J. Tranum-Jensen.** 1986. Membrane damage by pore-forming bacterial cytolysins. Microb. Pathog. **1:**5–14.
4. **Boehm, D. F., R. A. Welch, and I. S. Snyder.** 1990. Domains of *Escherichia coli* hemolysin (HlyA) involved in binding of calcium and erythrocyte membranes. Infect. Immun. **58:**1959–1964.
5. **Chen, L., and W. G. Coleman, Jr.** 1993. Cloning and characterization of the *Escherichia coli* K-12 *rfa*-2 (*rfaC*) gene, a gene required for lipopolysaccharide inner core synthesis. J. Bacteriol. **175:**2534–2540.
6. **Economou, A., W. D. O. Hamilton, A. W. B. Johnston, and J. A. Downie.** 1990. The *Rhizobium* nodulation gene *nodO* encodes a Ca^{2+}-binding protein that is exported without N-terminal cleavage and is homologous to haemolysin and related proteins. EMBO J. **9:**349–354.
7. **Felmlee, T., S. Pellett, and R. A. Welch.** 1985. The nucleotide sequence of an *Escherichia coli* chromosomal hemolysin. J. Bacteriol. **163:**94–105.
8. **Felmlee, T., and R. A. Welch.** 1988. Alterations of amino acid repeats in the *Escherichia coli* hemolysin affect cytolytic activity and secretion. Proc. Natl. Acad. Sci. USA **85:**5269–5273.
9. **Issartel, J.-P., V. Koronakis, and C. Hughes.** 1991. Activation of *Escherichia coli* prohaemolysin to the mature toxin by acyl carrier protein-dependent fatty acylation. Nature **351:**759–761.
10. **Kunkel, T. A.** 1985. Rapid and efficient site-specific mutagenesis without phenotypic selection. Proc. Natl. Acad. Sci. USA **82:**488–492.
11. **Ludwig, A., F. Garcia, S. Bauer, T. Jarchau, R. Benz, J. Hoppe, and W. Goebel.** 1996. Analysis of the in vivo activation of hemolysin (HlyA) from *Escherichia coli*. J. Bacteriol. **178:**5422–5430.
12. **Ludwig, A., T. Jarchau, R. Benz, and W. Goebel.** 1988. The repeat domain of *Escherichia coli* hemolysin (HlyA) is responsible for its Ca^{2+}-dependent binding to erythrocytes. Mol. Gen. Genet. **214:**553–561.
13. **Ludwig, A., A. Schmid, R. Benz, and W. Goebel.** 1991. Mutations affecting pore formation by haemolysin from *Escherichia coli*. Mol. Gen. Genet. **226:** 198–208.
14. **Ludwig, A., M. Vogel, and W. Goebel.** 1987. Mutations affecting activity and transport of haemolysin in *Escherichia coli*. Mol. Gen. Genet. **206:**238–245.
15. **Menestrina, G., C. L. Bashford, and C. A. Pasternak.** 1990. Pore-forming toxins: experiments with *S. aureus* alpha-toxin, *C. perfringens* delta-toxin, and *E. coli* haemolysin in lipid bilayers, liposomes and intact cells. Toxicon **28:**477–491.
16. **Moayeri, M.** 1996. Unpublished observations.
17. **Moayeri, M., and R. A. Welch.** 1994. Effects of temperature, time and toxin concentration on lesion formation by the *Escherichia coli* hemolysin. Infect. Immun. **62:**4124–4134.
18. **Moayeri, M., and R. A. Welch.** Chemical modification of *Escherichia coli* hemolysin cysteine substitution mutants. Submitted for publication.
19. **Pellett, S., D. F. Boehm, I. S. Snyder, G. Rowe, and R. A. Welch.** 1990. Characterization of monoclonal antibodies against the *Escherichia coli* hemolysin. Infect. Immun. **58:**822–827.
20. **Pellett, S., and R. A. Welch.** 1996. Unpublished data.
21. **Rowe, G. E.** 1994. A structure/function analysis of the *Escherichia coli* hemolysin: maturation and activation. Ph.D. thesis. University of Wisconsin, Madison, Wis.
22. **Stanley, P., L. Packman, V. Koronakis, and C. Hughes.** 1994. Fatty acylation of two internal lysine residues required for the toxic activity of the *Escherichia coli* hemolysin. Science **266:**1992–1996.
23. **Welch, R. A.** 1991. Pore-forming cytolysins of Gram-negative bacteria. Mol. Microbiol. **5:**521–528.
24. **Welch, R. A.** 1994. Holistic perspective on the *Escherichia coli* hemolysin, p. 351–364. *In* V. L. Miller, J. B. Kaper, D. Portnoy, and R. R. Isberg (ed.), Molecular genetics of bacterial pathogenesis. ASM Press, Washington, D.C.
25. **Welch, R. A., E. P. Dellinger, B. Minshew, and S. Falkow.** 1981. Hemolysin contributes to virulence of extra-intestinal *Escherichia coli* infections. Nature **294:**665–667.

Editor: P. E. Orndorff